RAA 2021 Vol. **21** No. **1**, 13(9pp) doi: 10.1088/1674-4527/20/1/13

http://www.raa-journal.org *http://iopscience.iop.org/raa*

Research in Astronomy and Astrophysics

Research on the readout noise suppression method for digital correlated double sampling

Wei Duan[1,2,3], Qian Song[1,2,3], Ming-Zhi Wei[1], Zhao-Wang Zhao[1,3], Wei Wang[1,3], Yu-Heng Zhang[1,3] and Zhi-Wei Feng[1,2,3,]

[1] National Astronomical Observatories, Chinese Academy of Sciences, Beijing 100101, China; *dw@bao.ac.cn*
[2] University of Chinese Academy of Sciences, Beijing 100049, China
[3] CAS Key Laboratory of Optical Astronomy, National Astronomical Observatories, Beijing 100101, China

Received 2020 May 30; accepted 2020 June 27

Abstract As the areas of CCD detectors and CCD mosaics have become larger and larger, the number of readout channels in astronomical cameras has increased accordingly to keep the image readout time within an acceptable range. For the large area cameras or the mosaic cameras, the analog Correlated Double Sampling (aCDS) circuit used in traditional astronomical cameras for suppressing readout noise is difficult to integrate into the camera controllers within the constraints of the space and energy consumption. Recently, digital CDS (dCDS) technology has been developed to solve this problem, which also offers novel analysis and noise suppression methods. In this study, a mathematical model is presented to conveniently analyze the frequency characteristic of a dCDS circuit, which is then simulated by a numerical method for investigating the noise suppression capability with different sampling weights. Importantly, using this model, the extreme point with lowest readout noise can be predicted for a certain dCDS model; and for a specific CCD readout frequency, readout noise can be suppressed by selecting the proper dCDS model. A testing system is then constructed for validating the efficiency of the proposed method.

Key words: instrumentation: detectors — methods: analytical — methods: numerical

1 INTRODUCTION

To detect weak signals from faint astronomical objects, the effective suppression of readout noises is a stringent requirement in designing the circuit of the controller of a scientific grade charge-coupled device (CCD) camera in astronomical applications (Howell 2006). A major source of readout noise is from CCD's output amplifier when it generates thermal electrons by its periodic resettings, and such noise is called kTC noise, e.g., $\sigma_{RN} \propto \sqrt{kT/C}$, where k is the Boltzmann constant, T is the temperature, and C is the capacitance (Boukhayma & Enz 2015). The correlated double sampling (CDS) method is an effective technique for reducing kTC noise during readout time (Caizzone et al. 2018), and is widely used in the CCDs controllers.

At present, the dual-slope integrator aCDS is widely used in CCD cameras for astronomical observations, which not only can suppress the kTC noise, but also suppress white noise and 1/f noise from CCD output amplifier (Janesick 2001). Because of the capability of suppression white noise and 1/f noise, it has high performance in readout noise suppression, and almost all the CCD cameras of the modern major telescopes in the world adopt dual-slope integrator aCDS circuits in the readout electronics, for instance, the UCAM controller developed by LICK Observatory. In this paper, the aCDS circuit means the dual-slope integrator aCDS circuit.

With the boom in large-area sky survey projects, large-area detectors and mosaic detectors will play a crucial role in future astronomy. To maintain an acceptable image readout time, these detectors surely will have a large number of readout channels. For example, the Zwicky Transient Facility (ZTF) is equipped with a 600-megapixel mosaic CCD, which is butted by sixteen chips of E2V Model CCD231-C6 (Dekany et al. 2020). The total number of readout channels is sixty-four. It is very difficult to design a small and power-efficienct controller for such a camera using aCDS technology.

With the development of semiconductor technology, digital CDS (dCDS) technology has become a possible alternative to aCDS (Dekany et al. 2020). By directly over-

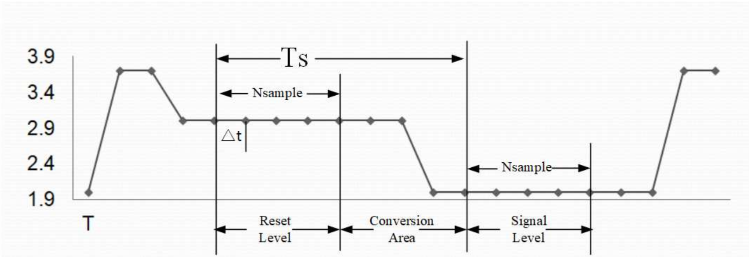

Fig. 1 Sampling diagram of Digital CDS.

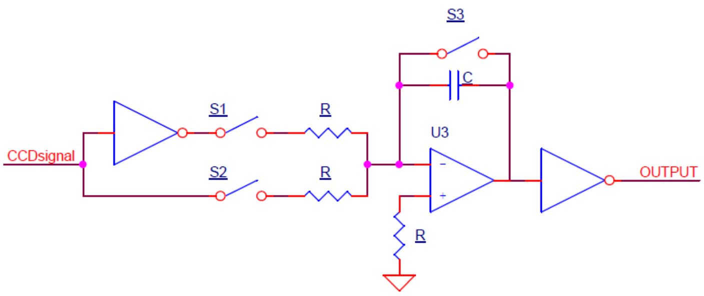

Fig. 2 Dual-slope integrator CDS circuit.

sampling readout signals from the CCD through a high-precision and high-speed Analog-to-Digital Converter (ADC) device, the digitized waveform of the signal with enough low noise can be obtained. A high-performance digital signal processor is used to eliminate the kTC noise by CDS method and generate an output image. Since one low power-consumption processor can deal with multiple readout channels, it can replace several aCDS circuits which contain many discrete components. Thus, both the volume occupation and the power consumption of the circuit are reduced. This technology has also been used in some astronomical CCD cameras. For example, the 10 k×10 k CCD of the Antarctica Survey Telescope (AST3), which has 16 readout channels, adopts the dCDS technology (Shang et al. 2012).

The technology of dCDS may solve the problems of space occupation and energy consumption, and it can also provide more choices to analyze the output amplifier noise of CCD and reduce the readout noise.

In this paper, a mathematical model of dCDS is built to analyze the dCDS circuit by numerical simulation, and a method for readout noise suppression is presented in Section 2. In Section 3, a set of systems that can realize the dCDS technology and the aCDS technology at the same time is developed, so as to test and verify the mathematical model as well as the noise suppression method proposed in Section 2. Section 4 summarizes the research of dCDS technology.

2 MATHEMATICAL MODEL OF THE DCDS CIRCUITS AND NOISE SUPPRESSION METHOD

The dCDS technology uses digital circuit instead of analog CDS circuit. The process of dCDS is shown in Figure 1, dCDS oversamples CCD readout signal by $N_{\rm sample}$ times in reset level and signal level, and uses digital signal processing method to achieve CDS.

Clapp (2012) generated the transfer function by simulating the noise components, which is complicated to get the transfer function. Stefanov & Murray (2014) deduced the transfer function by Z-transfer, in this way the analytical function is calculated. It is easy to know the frequency characteristic of dCDS, but if a different weight is needed for each sample, it is difficult to use this method. To overcome these problems, we propose to use a function shifting and averaging method as shown in Equation (1) to analyze the frequency characteristics, where a_k and b_k are the weight factors, $\triangle t$ is the sampling period ($1/f_{\rm sampling}$) and T_s is the shifting time shown in Figure 1. Equation (2) is the transfer function of Equation (1).

$$D_{\rm CDS} = \frac{\sum_{k=0}^{N_{\rm sample}-1} a_k \times V_{\rm CCD}(k \times \triangle t)}{\sum_{k=0}^{N_{\rm sample}-1} a_k} - \frac{\sum_{k=0}^{N_{\rm sample}-1} b_k \times V_{\rm CCD}(k \times \triangle t - T_s)}{\sum_{k=0}^{N_{\rm sample}-1} b_k} \quad (1)$$

$$H(f)=\frac{\sum_{k=0}^{N_{\mathrm{sample}}-1} a_k \times \exp(-j2\pi fk\times\triangle t)}{\sum_{k=0}^{N_{\mathrm{sample}}-1} a_k} - \frac{\sum_{k=0}^{N_{\mathrm{sample}}-1} b_k \times \exp(-j2\pi f(k\times\triangle t - T_s))}{\sum_{k=0}^{N_{\mathrm{sample}}-1} b_k} \tag{2}$$

The dCDS technology can easily obtain the transfer function, and we can analyze the frequency characteristic of the transfer function through numerical simulation, so as to understand the readout noise suppression.

2.1 Comparison between dCDS and aCDS

The aCDS circuit not only provides the function of CDS, but also acts as a low-pass filter. The aCDS circuit (see in Fig. 2) is widely used in astronomical cameras, and it can suppress the readout noise of CCD efficiently. Its transfer function can be expressed as Equation (3) (Hegyi & Burrows 1980) (where t_0 ($t_0=\triangle t\times N_{\mathrm{sample}}$) is the integrating time and T_s is the shifting time (Fig. 1)). The CDS circuit suppresses kTC noise and 1/f noise, its transfer function is $\sin^2(\pi \mathrm{fT_s})$ in Equation (3), while the low-pass filter ($\frac{4\times\sin^2(\pi \mathrm{ft_0})}{(\pi f t_0)^2}$ in Equation (3)) suppresses white noise and high-frequency noise.

$$|H_{\mathrm{aCDS}}(f)|^2=\frac{4\times\sin^2(\pi \mathrm{ft_0})}{(\pi \mathrm{ft_0})^2}\times\sin^2(\pi \mathrm{fT_s}) \tag{3}$$

The simplest model of dCDS is expressed as Equation (4), where a_k and b_k are 1. It is similar to an aCDS circuit, and the part $\sum_{k=0}^{N_{\mathrm{sample}}-1} V_{\mathrm{CCD}}(k\times\Delta t)/N_{\mathrm{sample}}$ describes the average value of the reset level, $\sum_{k=0}^{N_{\mathrm{sample}}-1} V_{\mathrm{CCD}}(k\times\Delta t-T_s)/N_{\mathrm{sample}}$ describes the average value of the signal level. The transfer functions of these two parts are same except for the shifting time (T_s), the difference of these two parts is CDS.

$$D_{\mathrm{CDS}}=\frac{\sum_{k=0}^{N_{\mathrm{sample}}-1} V_{\mathrm{CCD}}(k\times\triangle t)}{N_{\mathrm{sample}}}-\frac{\sum_{k=0}^{N_{\mathrm{sample}}-1} V_{\mathrm{CCD}}(k\times\triangle t-T_s)}{N_{\mathrm{sample}}} \tag{4}$$

$$|H_{\mathrm{dCDS}}(f)|^2=4\times\frac{(\sum_{k=0}^{N_{\mathrm{sample}}-1}\sin(2\pi fk\times\triangle t))^2+(\sum_{k=0}^{N_{\mathrm{sample}}-1}\cos(2\pi fk\times\triangle t))^2}{N_{\mathrm{sample}}^2}\times\sin^2(\pi \mathrm{fT_s}) \tag{5}$$

Equation (5) is the transfer function of the simplest dCDS circuit, its frequency characteristic is related to two parameters of Δt and N_{sample}, where Δt is the sampling period, and N_{sample} is the number of sampling related to the integrating time ($t_0=\Delta t\times N_{\mathrm{sample}}$). A low-pass filter must be used to avoid aliasing in according to Δt by sampling theory.

We analyze the influence of N_{sample} on the frequency characteristic while keeping the same sampling frequency $f_{\mathrm{sampling}}=10\,\mathrm{MHz}$ ($\Delta t=100\,\mathrm{ns}$). Figure 3 shows the frequency characteristic with different N_{sample}, when sampling frequency is fixed in 10 MHz. It can clearly be seen that as N_{sample} increases, the bandwidth of the band-pass filter decreases and the peak of the filter shifts to the low frequency area, which is similar to aCDS circuit.

According to the above analysis, the bandwidth and peak frequency of the digital band-pass filter in dCDS circuit are only related to the integrating time ($\Delta t\times N_{\mathrm{sample}}$). The longer the integrating time, the narrower the bandwidth of band-pass filter, and the lower the peak frequency.

The frequency characteristic of dCDS are obtained using Equation (5), where the readout frequency of CCD is 50 kHz and the sampling frequency is 10 MHz, so N_{sample} is about 100. Figure 4 shows a comparison of frequency characteristic of aCDS and dCDS, which indicates that the two CDS technologies have the same frequency characteristic if the integrating time $t_0(t_0=N_{\mathrm{sample}}\times\Delta t)$ and shifting time T_s are the same in both CDS circuits.

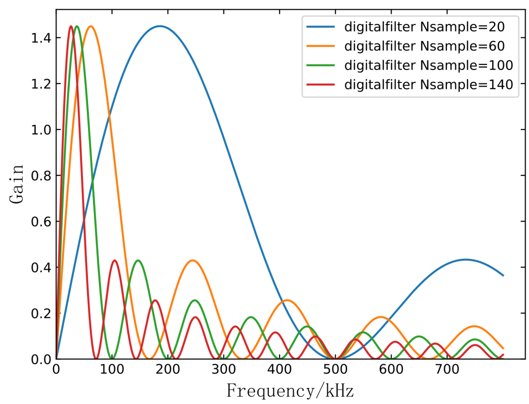

Fig. 3 Frequency characteristic of dCDS with different N_{sample}, when sampling frequency is 10 MHz($\Delta t=100\,\mathrm{ns}$).

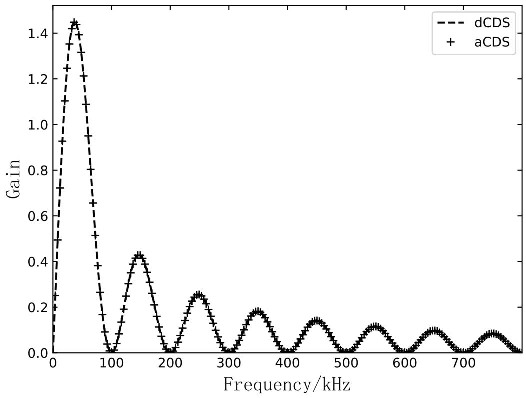

Fig. 4 Frequency characteristic comparison of aCDS and dCDS, when $N_{\mathrm{sample}} \times \Delta t = t_0 = 10\,\mathrm{ms}$.

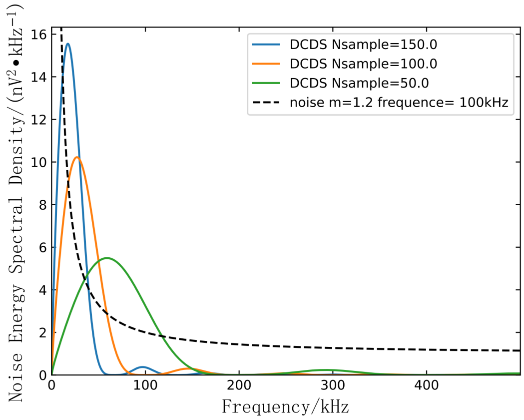

Fig. 5 The noise energy spectral density after dCDS with different N_{sample}.

2.2 The Method to Find the Lowest Readout Noise Point in the Simplest dCDS Model

The kTC noise is an extremely low frequency noise; its frequency is about 2.5×10^{-6} Hz (Janesick 2001), which is easy to filter out. The performance of CDS circuit is determined by the capability to suppress white noise and 1/f noise, which are the dominant noises in CCD output amplifier. The noise energy spectral density of output amplifier is shown in Equation (6) (Janesick 2001), where W_{CCD} is white noise, (constant in all bands), f_c is noise corner frequency of 1/f noise, and the parameter m characterizes the slope of the 1/f noise spectrum, ranging from 1 to 2. In our mathematical model, we choose $m = 1.2$ and $f_c = 100\,\mathrm{kHz}$.

$$N_{\mathrm{CCD}}{}^2 = W_{\mathrm{CCD}}{}^2(f) \times (1 + (f_c/f)^m) \qquad (6)$$

In Section 2.1, we have described the mathematical model of the simplest dCDS, where different N_{sample} means different CCD readout frequencies ($f_{\mathrm{readout}} \approx \frac{1}{(2\times N_{\mathrm{sample}}+50)\times \Delta t}$), the transfer functions with different N_{sample} are different.

Also, we find that as the bandwidth becomes narrower in Figure 3, the high frequency noise and white noise are suppressed, but the 1/f noise increases and gradually becomes dominant as the peak of the filter shifts to the low frequency area. Because the readout noise mainly consists of white noise and 1/f noise together, there is an extreme point where the readout noise of a CCD is at its lowest.

Figure 5 shows the noise energy spectral density after dCDS (the dotted line is the noise energy spectral density of the N^2_{CCD} ($m = 1.2$, $f_c = 100\,\mathrm{kHz}$)). The readout noise energy can be obtained by integrating the noise energy spectral density curve shown in Figure 6, where we can see the minimum readout noise frequency (MRNF) of dCDS circuit, i.e. where the readout noise is the lowest. When

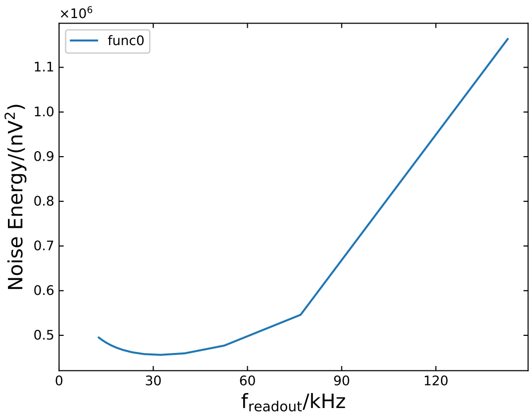

Fig. 6 Noise energy vs f_{readout} with the simplest dCDS model when CCD noise model is $W_{\mathrm{CCD}} = 1\,\mathrm{nV}$, $f_c = 100\,\mathrm{kHz}$, $m = 1.2$.

$f_{\mathrm{readout}} \approx 29\,\mathrm{kHz}$, the simplest dCDS model has the least readout noise energy.

This method can also be used to analyze the frequency characteristic of dCDS with different weights, and the MRNF can be found for different CCD noise models.

2.3 The Method to Suppress the Readout Noise at a Certain CCD Readout Frequency

The simplest dCDS model analyzed above assumes the same weight factors, but one of the advantages of dCDS is changing the characteristics of dCDS circuit by choosing a different weight for each sampling point. So, the performance of dCDS with different weights is studied here using the method above, then the MRNF could be found out.

Gach et al. (2003) found that samples near the conversion area (from reset level to signal level in Fig. 1) are correlated, so choosing the samples near this area can

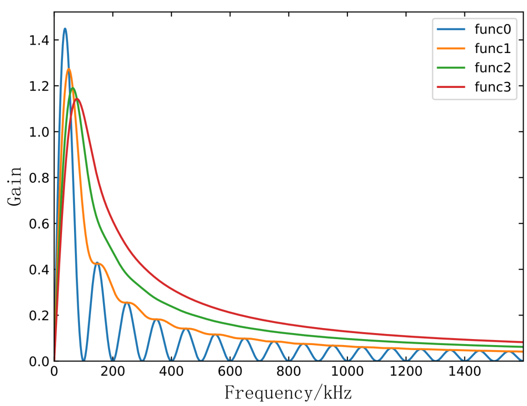

Fig. 7 Frequency characteristic of dCDS model with different weight Function when $N_{\text{sample}} = 100$, Func0 means weight factor $a_k = b_k = 1$, Func1 means the weight factor $a_k = k$, $b_{N_{\text{sample}}-k} = k$, Func2 means the weight factor $a_k = k^2$, $b_{N_{\text{sample}}-k} = k^2$ and Func3 means the weight factor $a_k = k^3$, $b_{N_{\text{sample}}-k} = k^3$.

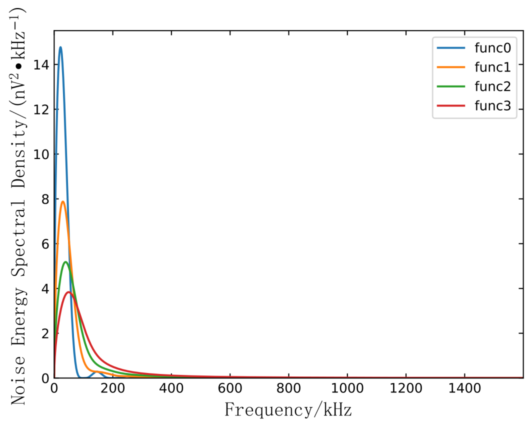

Fig. 8 Noise energy spectral density after dCDS, when f_{readout} is 40 kHz ($N_{\text{sample}} = 100$) and the CCD noise model is W_{CCD} = 1nV, $f_c = 100$kHz and $m = 1.2$, Func0 means weight factor $a_k = b_k = 1$, Func1 means the weight factor $a_k = k$, $b_{N_{\text{sample}}-k} = k$, Func2 means the weight factor $a_k = k^2$, $b_{N_{\text{sample}}-k} = k^2$ and Func3 means the weight factor $a_k = k^3$, $b_{N_{\text{sample}}-k} = k^3$.

result in lower readout noise, and CCD readout noise can be suppressed by setting high weight for sampling points near the conversion area of the dCDS circuit.

The analysis of different weights can also use Equation (1) mentioned above, which is the mathematical model of the dCDS with weight, where a_k and b_k are a mirror function, $a_k = b_{N_{\text{sample}}-k}$. Equation (2) is the transfer function. We choose power function (k^n) as the mirror function for a_k and b_k, if n is 0, $a_k = b_k = 1$, with increasing n, the sampling point near the conversion area has higher weight. Here, four models with $n = 0, 1, 2$

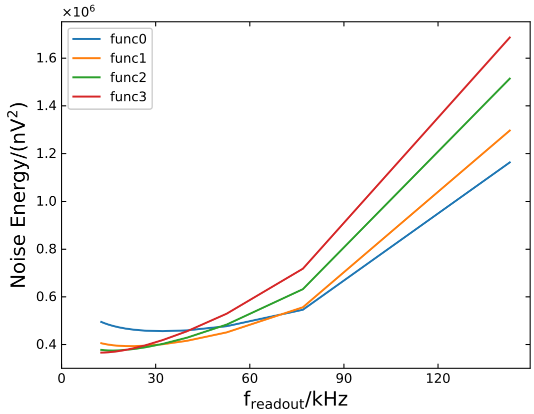

Fig. 9 Noise energy vs f_{readout}, when the CCD noise model is W_{CCD} =1nV, $f_c = 100$ kHz and $m = 1.2$, Func0 means weight factor $a_k = b_k = 1$, Func1 means the weight factor $a_k = k$, $b_{N_{\text{sample}}-k} = k$, Func2 means the weight factor $a_k = k^2$, $b_{N_{\text{sample}}-k} = k^2$ and Func3 means the weight factor $a_k = k^3$, $b_{N_{\text{sample}}-k} = k^3$.

and 3 are built as the transfer function curves shown in Figure 7 (where func0 means $n = 0$, and so on) when CCD readout frequency (f_{readout}) is 40 kHz. It is found as the increasing of n, the peak point of the filter shifts to right direction, which is beneficial for suppressing 1/f noise, but the bandwidth of filter is extended to leave more white noise, thus the total noise must be analyzed to find out the point with the lowest readout noise. Figure 8 shows the noise energy spectral density passing dCDS filters with different weights when f_{readout} is 40 kHz, the readout noise energy can be calculated by integrating the curve.

Figure 9 shows the relationship of the readout noise energy vs f_{readout} (related to N_{sample}). When n increases, the readout noise energy decreases when CCD readout frequency is low, but when CCD readout frequency becomes high, the readout noise energy increases.

Then we try two more weight models, Gaussian-shaped weight model and exponential function model (e^k), the readout noise ($m = 1.2$, $f_c = 100$ kHz are used in the noise model) using Gaussian-shaped weights is similar to power function (k^n). If the exponential function model is used, the readout noise is higher because the white noise can pass the system in all bands, as the weight of the sample near the conversion area is too high and the bandwidth of transfer function of dCDS is too wide.

The analysis above is based on the noise model with $m = 1.2$ and $f_c = 100$ kHz We now change m and f_c and then analyze the readout noise theoretically. At first, when f_c becomes to 200kHz and m is still 1.2, the readout noise energy at the different f_{readout} is shown on the left of Figure 10. Then we change m to 1.4 and f_c is still 100 kHz,

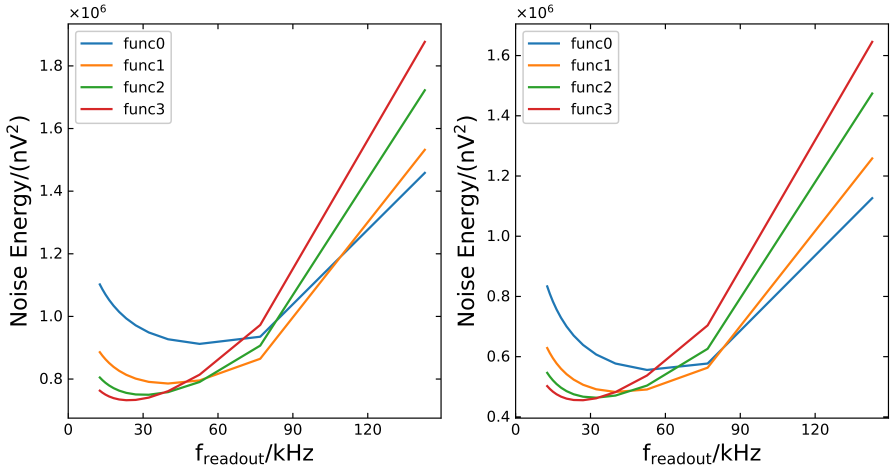

Fig. 10 Left figure is the noise energy ($m = 1.2$, $f_c = 200\,\mathrm{kHz}$) and right figure is ($m = 1.4$, $f_c = 100\,\mathrm{kHz}$), Function is the dCDS model, Func0 means weight factor $a_k = b_k = 1$, Func1 means the weight factor $a_k = k$, $b_{N_{\mathrm{sample}}-k} = k$, Func2 means the weight factor $a_k = k^2$, $b_{N_{\mathrm{sample}}-k} = k^2$ and Func3 means the weight factor $a_k = k^3$, $b_{N_{\mathrm{sample}}-k} = k^3$.

the readout noise energy with different f_{readout} is shown on the right of Figure 10. Under the above conditions, the dCDS with different weights can suppress the readout noise more efficiently than using the same weight in low readout frequency area, but in high readout frequency area, the dCDS with same weight has the best performance.

Through the analysis, we find that the MRNF can be calculated. When n (function k^n) increases, the MRNF is lower, and the system has lower readout noise in low readout frequency area, but in high frequency area, the performance is the best when n is 0.

We also found that the capability to suppress the readout noise with the different weight factors is different with the same f_{readout}, func1 is the best filter when f_{readout} is 67kHz, but func2 or func3 is the best filter when f_{readout} is 40 kHz.

In astronomical observations, when a certain dCDS model is used, we can find the MRNF to make the camera work with the lowest readout noise by the method above; the method also can be used to find the optimized dCDS model to get the lower readout noise for a certain CCD readout frequency. In Section 3, we will compare test results with the theoretical results.

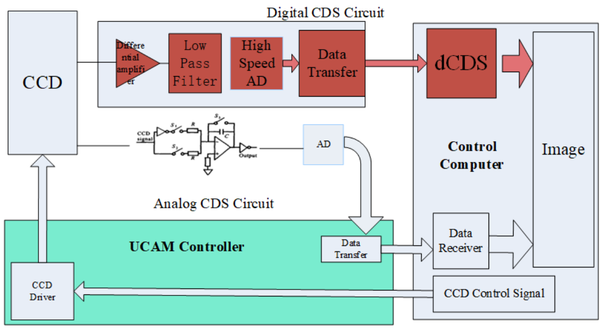

Fig. 11 The schematic diagram of the performance test system.

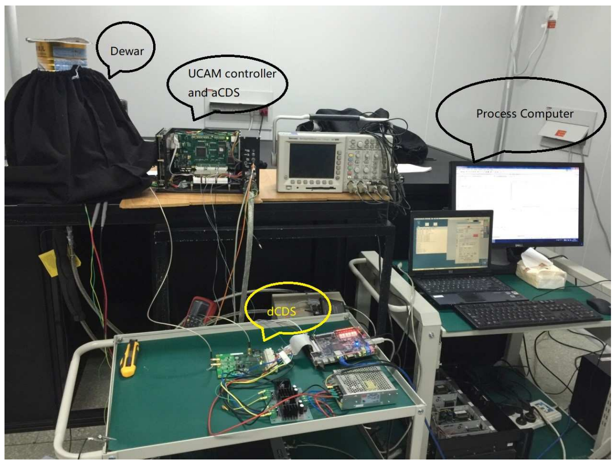

Fig. 12 The performance test system.

3 PERFORMANCE TEST SYSTEM AND ANALYSIS OF TEST RESULT

3.1 Performance Test System

A schematic diagram of the performance test system is shown in Figure 11, which supports both dCDS and aCDS technologies at the same time. The system uses the CCD42–40 chip made by E2V company with two outputs. One of the CCD outputs is connected to the aCDS circuit, the other one is connected to dCDS circuit, and the rest of circuits are shared. Figure 12 is a photo of the actual performance test system, which includes a UCAM

Fig. 13 Image of digital CDS.

Table 1 Readout Noise with Different CDS Circuit

f_{readout}	dCDS	aCDS
50 kHz	3.8e$^-$	2.7e$^-$
100 kHz	5.7e$^-$	4.1e$^-$

controller and a separate dCDS circuit. UCAM controller contains the driver circuit of CCD and an aCDS circuit connected to one of the CCD output channels. The dCDS circuit is integrated by us, and includes a high-speed ADC (AD7626, 10 MHz, 16 bit), which oversamples the CCD output channel to get the digital readout signal. The digital CCD waveform is transmitted to a PC via a gigabit network by FPGA, then the CDS calculation is implemented on a PC, and finally the image is obtained, as shown in Figure 13.

3.2 Readout Noise Comparison between aCDS and dCDS

On this test system, we first compared the readout noise between aCDS and dCDS; the results are listed in Table 1. When the readout frequency is 50 kHz, the readout noise from the camera is $3.8e^-$ using dCDS, and $2.7e^-$ using aCDS. When the readout frequency is 100 kHz, the readout noise from the camera is $5.7e^-$ using dCDS, and $4.1e^-$ using aCDS. As a comparison, the readout noise of the test system using the dCDS circuit is close to the readout noise of the UCAM controller using aCDS circuit. This result is consistent with the theoretical calculation and validates the efficiency of dCDS technology used in astronomical observations.

3.3 Testing for the Method to Find the MRNF for a Certain dCDS Model

We then analyzed the relationship between the readout noise and f_{readout} of the test platform. The results are shown in Figure 14 while all weight factors are 1 and the CCD noise model here is $W_{\mathrm{CCD}} = 1\,\mathrm{nV}$, $m = 1.25$ and $f_c = 65\,\mathrm{kHz}$. The left figure shows the readout noise energy calculated using theoretical method of dCDS circuit shown in Section 2, the right figure shows the measured readout noise of the test system using dCDS circuit. The MRNF obtained from both the theoretical calculation and actual measurement are at the position of $f_{\mathrm{readout}} \approx$ 28.5 kHz ($t_0 = 15\,\mu\mathrm{s}$), and the readout noise is measured to be $3.5e^-$ at this MRNF.

We checked the MRNF of aCDS circuit in the test system, when $f_{\mathrm{readout}} \approx 30$ kHz ($t_0 = 16\,\mu\mathrm{s}$), the readout noise is the lowest, which indicates that the MRNF of this CCD chip is generally at the same value for both aCDS and dCDS circuits.

The above results demonstrate that the MRNF with the lowest readout noise could be calculated by the proposed method.

3.4 Testing for the Method to Suppress the Readout Noise at a Specific CCD Readout Frequency

Figure 15 shows the readout noise with different weight factors. In Figure 15, each curve corresponds to different n (weight factor is k^n). On comparison, the theoretical result and the measured result have the same characteristics.

We confirm that the proposed method can be used to optimize the weight factors for a given special f_{readout} as shown in Figure 15. The left figure shows the readout noise energy with different weight factors calculated by theoretical method, and the right figure shows the measured readout noise of the test system using dCDS circuit. In these figures, each curve means a different weight factor (k^n). By comparison, it is found that the theoretical results are identical to the measured results. Thus, we can predict the optimized weight factor using the theoretical method as shown in the left figure, which is further confirmed by Table 2, when f_{readout} = 67 kHz, the theoretical readout noise energy and the measurable readout noise show same trend, and we can infer that the optimized weight factor is $n = 0$; and for f_{readout} = 28 kHz, the theoretical readout noise energy and the measurable readout noise also show same trend, and the optimized weight factor is $n = 1$ for the lowest readout noise.

Therefore, we can use the mathematical model to find out which dCDS model will optimize the readout noise for a certain readout frequency in astronomical applications.

4 CONCLUSIONS

CDS technology plays an important role in the readout noise suppression of astronomical CCD controllers. dCDS

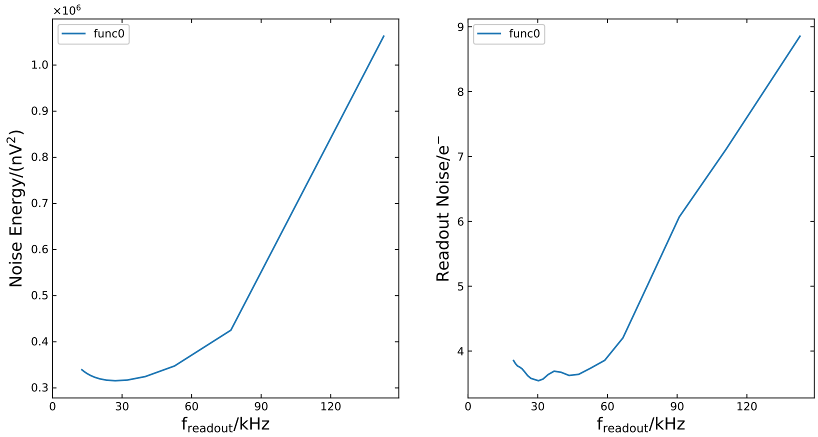

Fig. 14 The left figure is readout noise energy by theoretical calculating (CCD noise model is $W_{\mathrm{CCD}} = 1\,\mathrm{nV}$, $m = 1.25$ and $f_c = 65\,\mathrm{kHz}$) and the right figure is measurement readout noise, Fucn0 is used as dCDS model ($a_k = b_k = 1$).

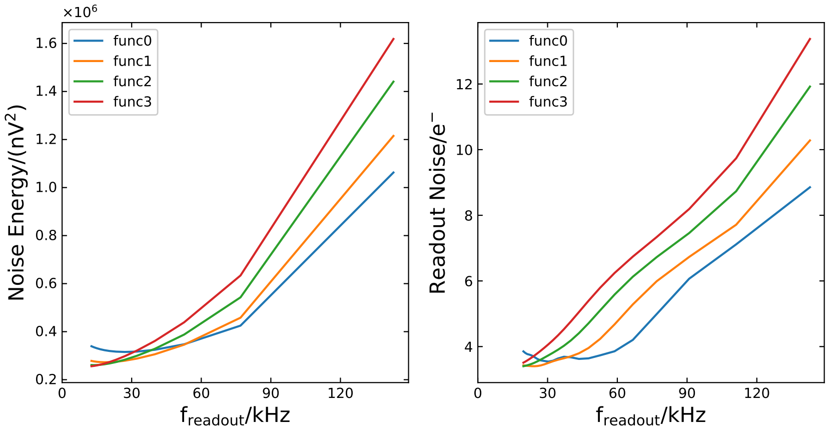

Fig. 15 The left figure is readout noise energy by theoretical calculating (CCD noise model is $W_{\mathrm{CCD}} = 1\,\mathrm{nV}$, $m = 1.25$ and $f_c = 65\,\mathrm{kHz}$) and the right figure is measurement readout noise, Func0 means weight factor $a_k = b_k = 1$, Func1 means the weight factor $a_k = k$, $b_{N_{\mathrm{sample}}-k} = k$, Func2 means the weight factor $a_k = k^2$, $b_{N_{\mathrm{sample}}-k} = k^2$ and Func3 means the weight factor $a_k = k^3$, $b_{N_{\mathrm{sample}}-k} = k^3$.

Table 2 Theoretical Readout Noise Energy vs Measureable Readout Noise

Weight Factor	$f_{\mathrm{readout}} = 67\,\mathrm{kHz}$		$f_{\mathrm{readout}} = 40\,\mathrm{kHz}$		$f_{\mathrm{readout}} = 28\,\mathrm{kHz}$	
	TRDP/(nV)^2	MRD/e^-	TRDP/(nV)^2	MRD/e^-	TRDP/(nV)^2	MRD/e^-
Func0=1	386850	4.129	324580	3.678	315263	3.552
Func1=k	404613	5.408	305920	3.676	281349	3.447
Func2=k^2	470358	6.324	328750	4.196	287669	3.656
Func3=k^3	543734	6.952	361274	4.830	304455	3.971

[a] TRDP (Theoretical readout noise energy); [b] MRD (Measurable readout noise).

is more flexible to use more kinds of CDS models with different weight factors to process CCD signals than aCDS.

In this study, for a dCDS model, we can find the MRNF based on the CCD noise model, where the readout noise is the lowest. In the performance test system, the MRNF by theoretical calculating is about 28.5 kHz, which was proven by the measured results from the dCDS circuit and aCDS circuit, thus the astronomical camera can get best performance at this readout frequency.

We also find that for different CCD readout frequencies the readout noise can be suppressed by using different dCDS models, the method above can help to find the optimized model for a certain readout frequency. For example, when $f_{\mathrm{readout}} \approx 28\,\mathrm{kHz}$, Func1 is the best dCDS model, but when $f_{\mathrm{readout}} \approx 67\,\mathrm{kHz}$, Func0 is the best one as discussed in Section 3. Therefore, an astronomer can use the theoretical calculation to choose the best dCDS model to process the CCD signal to lower the readout noise, when the CCD readout frequency of the astronomical camera is chosen.

In astronomical observations, scientists can select the dCDS model according to the CCD noise model by theoretical analysis, as was proved by the testing systems; and for different readout frequencies, they also can choose the optimized dCDS model to decrease the readout noise by theoretical analysis. So, the most suitable dCDS model for a certain application can easily be found.

There is still possibility to further optimize the hardware system on the test system, for example, the circuit between CCD output amplifier to ADC needs to be carefully tuned to get better performance. In addition, the dCDS technology has great flexibility due to oversampling of CCD signal, so the system can achieve better performance by adjusting the parameters of filter design. Furthermore, we can also use intelligent algorithms to improve the anti-jamming ability, reduce the requirements of electromagnetic environment. Thus, dCDS is becoming a promising technology for large CCD control systems.

Acknowledgements Thanks to Yi Hu, Zhiying Huo and Xianyong Bai for their helpful discussion, and thanks to the reviewer for the improvement of this paper. This research is supported by the National Natural Science Foundation of China (Grant No. 11403050).

References

Boukhayma, A., & Enz, C. 2015, in 2015 IEEE 13th International New Circuits and Systems Conference (NEWCAS), IEEE, 1

Caizzone, A., Boukhayma, A., & Enz, C. 2018, in 2018 16th IEEE International New Circuits and Systems Conference (NEWCAS), IEEE, 22

Clapp, M. J. 2012, in Society of Photo-Optical Instrumentation Engineers (SPIE) Conference Series, 8453, High Energy, Optical, and Infrared Detectors for Astronomy V, 84531D

Dekany, R., Smith, R. M., Riddle, R., et al. 2020, PASP, 132, 038001

Gach, J. L., Darson, D., Guillaume, C., et al. 2003, PASP, 115, 1068

Hegyi, D. J., & Burrows, A. 1980, AJ, 85, 1421

Howell, S. B. 2006, Handbook of CCD Astronomy, 5 (Cambridge, UK: Cambridge Univ. Press)

Janesick, J. R. 2001, Scientific charge-coupled devices (Bellingham, WA: SPIE Optical Engineering Press)

Shang, Z., Hu, K., Hu, Y., et al. 2012, in Society of Photo-Optical Instrumentation Engineers (SPIE) Conference Series, 8448, Proc. SPIE, 844826

Stefanov, K. D., & Murray, N. J. 2014, Electronics Letters, 50, 1022